Bioorganic & Medicinal Chemistry 19 (2011) 7690–7697

Contents lists available at SciVerse ScienceDirect

Bioorganic & Medicinal Chemistry

journal homepage: www.elsevier.com/locate/bmc

Camptothecin (CPT) directly binds to human heterogeneous nuclear ribonucleoprotein A1 (hnRNP A1) and inhibits the hnRNP A1/topoisomerase I interaction

Daisuke Manita, Yuzuru Toba, Yoichi Takakusagi [†], Yuki Matsumoto, Tomoe Kusayanagi, Kaori Takakusagi, Senko Tsukuda, Kazunori Takada, Yoshihiro Kanai, Shinji Kamisuki, Kengo Sakaguchi, Fumio Sugawara [*]

Department of Applied Biological Science, Faculty of Science and Technology, Tokyo University of Science, 2641 Yamazaki, Noda, Chiba 278-8510, Japan

ARTICLE INFO

Article history:
Received 9 September 2011
Accepted 29 September 2011
Available online 5 October 2011

Keywords:
Camptothecin
Topoisomerase I
QCM
SPR
hnRNP A1
Hrb87F
Drosophila melanogaster

ABSTRACT

Camptothecin (CPT) is an anti-tumor natural product that forms a ternary complex with topoisomerase I (top I) and DNA (CPT-top I-DNA). In this study, we identified the direct interaction between CPT and human heterogeneous nuclear ribonucleoprotein A1 (hnRNP A1) using the T7 phage display technology. On an avidin-agarose bead pull down assay, hnRNP A1 protein was selectively pulled down in the presence of C20-biotinylated CPT derivative (CPT-20-B) both in vitro and in vivo. The interaction was also confirmed by an analysis on a quartz-crystal microbalance (QCM) device, yielding a K_D value of 82.7 nM. A surface plasmon resonance (SPR) analysis revealed that CPT inhibits the binding of hnRNP A1 to top I (K_D: 260 nM) in a non-competitive manner. Moreover, an in vivo drug evaluation assay using *Drosophila melanogaster* showed that the knockout of the hnRNP A1 homolog Hrb87F gene showed high susceptibility against 5–50 μM of CPT as compared to a wild-type strain. Such susceptibility was specific for CPT and not observed after treatment with other cytotoxic drugs. Collectively, our data suggests that CPT directly binds to hnRNP A1 and non-competitively inhibits the hnRNP A1/top I interaction in vivo. The knockout strain loses the hnRNP A1 homolog as a both CPT-binding partner and naïve brakes of top I, which enhances the formation of the CPT-top I-DNA ternary complexes and subsequently sensitizes the growth inhibitory effect of CPT in *D. melanogaster*.

1. Introduction

Camptothecin (CPT) is an anti-tumor natural product that was isolated from *Camptotheca acuminata* by Wall et al.[1] CPT forms ternary complex with topoisomerase I (top I) and DNA (CPT-top I-DNA) and inhibits the DNA relaxation by top I in the submicromolar concentration range,[2,3] which result in apoptotic cell death or delay of tumor growth in live animals. Whilst, there are the numbers of reports that assume the presence of alternative molecular target(s) other than top I or factors that modulate the susceptibility of CPT both in vitro and in vivo.[4–13] Discovery of unidentified binding partner of CPT would be of interest to understanding further insights into the mode of action of CPT at the molecular level.

Previously, we reported the screening of a library of T7 phage-displayed peptides that recognizes CPT.[14] In the experiment, we identified a CPT-recognizing short peptide (15-mer; NSASRGG SQRGRGEH) using a C20-biotinylated CPT (CPT-20-B, Fig. 1A).[14,15] This amino acid sequence displayed similarity to part of a region in top I containing Arg364 where CPT binds directly and forms a ternary complex with DNA.[14,16] In our further analysis of sequence similar to the 15-mer peptide, there were a large number of potential hits in the protein database, suggesting the presence of unidentified CPT-binding protein. Among them, we focused on a splicing factor human heterogeneous nuclear ribonucleoprotein A1 (hnRNP A1). The hnRNP A1 is known to form pre-mRNA complex with other subtype of hnRNPs and pre-mRNA-binding proteins and play a role in pre-mRNA splicing and mRNA metabolisms in nucleus.[17,18] Interestingly, it has been reported that a series of RRM proteins including hnRNP A1, directly bind to the cap region (215–433) of human top I

Abbreviations: CPT, camptothecin; CPT-20-B, C20-biotinylated camptothecin; hnRNP, heterogeneous nuclear ribonucleoprotein; Hrb87F, heterogeneous nuclear ribonucleoprotein 87F; QCM, quartz-crystal microbalance; RRM, RNA recognition motif; SPR, surface plasmon resonance; top, topoisomerase.

* Corresponding author. Tel.: +81 471 24 1501x3400; fax: +81 471 23 9767.
E-mail address: sugawara@rs.noda.tus.ac.jp (F. Sugawara).
† Present address: National Cancer Institute, National Institutes of Health, Bethesda, MD, USA.

0968-0896/$ - see front matter © 2011 Elsevier Ltd. All rights reserved.
doi:10.1016/j.bmc.2011.09.059

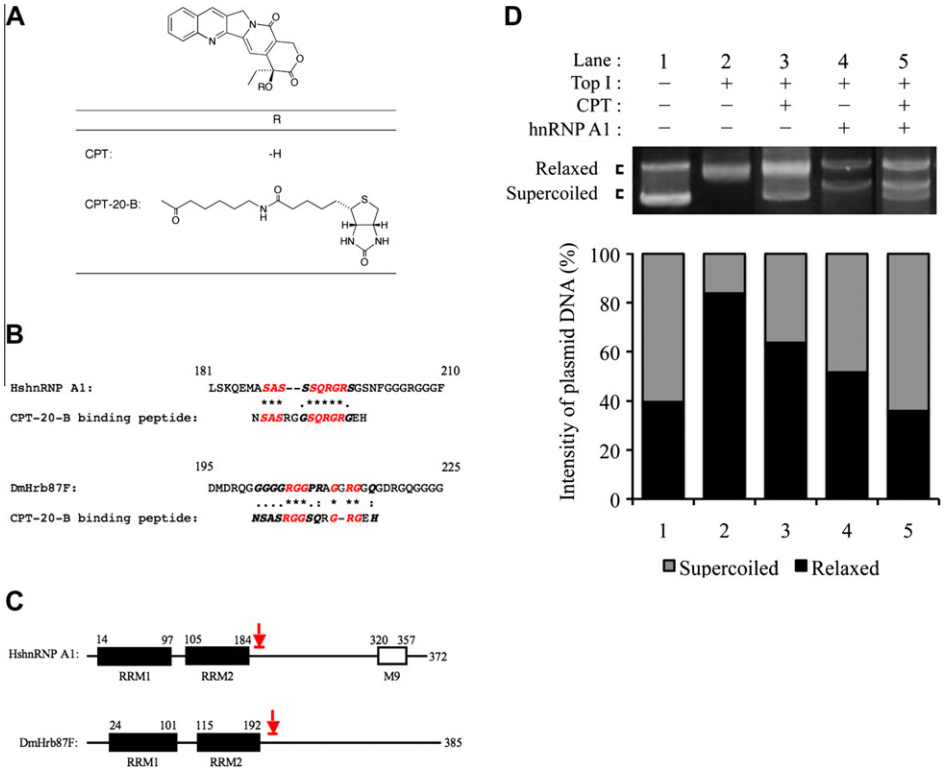

Figure 1. Structure of camptothecins (CPTs) and similarity between the CPT-recognizing 15-mer peptide and hnRNP A1 or Hrb87F. (A) Structure of CPT and CPT-20-B. (B) Similarity of amino acid sequence between the 15-mer peptide and hnRNP A1 (S188–R196) or Hrb87F (202G–216Q). (C) Schematic representation of full length hnRNP A1 and Hrb87F and the similarity site (indicated by the red arrows). RRM; RNA recognition motif, M9; cellular distribution signal. (D) The supercolided DNA relaxation assay. Plasmid (lane 1). Plasmid + top I (lane 2), + top I and CPT (lane 3), + top I and hnRNP A1-GST (lane 4), + top I and CPT and hnRNP A1-GST (lane 5).

via two tandem RRM domains and decrease CPT-induced DNA cleavage, which could regulate the activity of top I.[19–21]

In this study, we verified the interaction between CPT and hnRNP A1 using an avidin-agarose bead pull down assay and a quartz-crystal microbalance (QCM) biosensor-based interaction analysis. We also assessed the effect of CPT for hnRNP A1/top I interaction using a surface plasmon resonance (SPR) analysis and fitting for binding model. Furthermore, we elucidated the change of growth inhibitory effect of CPT in vivo by the use of a *Drosophila*-based drug evaluation system, focusing on the hnRNP A1/top I interaction.

2. Materials and methods

2.1. Materials

HeLa cell was obtained from Cell Resource Center for Biomedical Research Institute of Development, Aging and Cancer (Tohoku University, Sendai, Japan). DMEM was purchased from Nacalai Tesque Co. Ltd (Kyoto, Japan). The *Hrb87F* gene mutants (*P*-element insertion) of *Drosophila*, $Hrb87F^{KG02089}$ (stock ID 14414) and $Hrb87F^{BG02743}$ (stock ID 12869) were obtained from Bloomington Drosophila Stock Center (BDSC) [http://flystocks.bio.indiana.edu/]. Cloning System was obtained from Novagen (Madison, WI). pGEX-6P-1 vector, GSTrap FF column and Glutathione Sepharose™ 4B were purchased from GE Healthcare (Amersham, UK). RNA extraction reagent (Sepasol-RNA Super G) was from nacalai tesque. Restriction enzyme *Bam*HI and *Xho*I were obtained from TOYOBO (Osaka, Japan). T4 ligase was from Promega (Madison, WI). PCR reagent was obtained from TaKaRa (Tokyo, Japan). Avidin-agarose beads was from Sigma-Aldrich (St Louis, MO). An anti-hnRNP A1 mouse monoclonal IgG_{28} antibody and goat anti-mouse IgG antibody-AP conjugate was obtained from Santa Cruz Biotechnology Inc. (Santa Cruz, CA), Nacalai Tesque, respectively.

2.2. Drugs

Irinotecan was kindly provided from Yakult Co. Ltd (Tokyo, Japan) and Dai-ichi Pharmaceutical Co. Ltd (Tokyo, Japan). Camptothecin and cysplatin were obtained from Tokyo Kasei Co. Ltd (Tokyo, Japan). Paclitaxel was purchased from Hoechst Marion Roussel Co. Ltd (Romainville, France). Doxorubicin was obtained from Toronto Research Chemicals Inc. (North York, ON). Bleomycin was obtained from Wako (Tokyo, Japan).

The synthesis of CPT-20-B (Fig. 1A) was described previously.[15]

2.3. Expression of recombinant protein using an *E. coli* cloning system

The hnRNP A1 gene was isolated from a cDNA library of HeLa cells. Briefly, total RNA was extracted using Sepasol-RNA Super G (Nacalai Tesque) and then reverse transcription was performed using ReverTra Ace® qPCR RT Kit (TOYOBO) with a random primer according to the manufacture's instructions. The gene of hnRNP A1 was amplified by PCR using primers 5′-GGATCCATGTCTAAGTCAG AGTCTCCT-3′ (PM1) and 5′-CTCGAGTTAAAATCTTCTGCCACTGC CAT-3′ (PM2), and then inserted into the multi-cloning site of pGEX-6P-1 vector (GE Healthcare). Competent BL21 (DE3) pLysS cells (Novagen) were then transformed with the plasmid.

The gene of cap region (215–433) of top I gene was amplified from cDNA clones top I (TOYOBO) by PCR using primers 5′-AAGGATCCATCAAGTGGAAATTCCTAGAACAT-3′ (PM3) and 5′-AACTCGAGTTATGAACTAGGGTTAAGCATGATGTA-3′ (PM4). The PCR product was then inserted into pET-28a(+) vector (Novagen).

Competent Rosetta 2 (DE3) pLysS Competent cells (TOYOBO) were then transformed with the plasmid.

Single colonies were transferred into LB medium containing 1% glucose, 50 μg/ml of ampicillin (Amp, for hnRNP A1) or 30 μg/ml of kanamycin (Km, for cap region of top I) and 34 μg/ml of chloramphenicol (Cm), and cultured at 37 °C, overnight. The cells were then transferred to large scale of LB medium containing 1% glucose, antibiotics and cultured for 3 h at 37 °C. IPTG was added to the culture medium at a final concentration of 1 mM and the cells were incubated for a day at 20 (hnRNP A1) or 25 (cap region of top I) °C to induce protein expression. The cells were harvested by centrifugation at 5000*g* for 10 min at 4 °C.

2.4. Preparation of HeLa cell and *E. coli* soluble lysates

HeLa cells were cultured in DMEM supplemented with 10% fetal calf serum in a humidified chamber at 37 °C containing 5% CO_2. The 10^7 of cultured HeLa cells were washed with PBS twice and then treated with a cell extraction buffer (25 mM Tris–HCl, pH 8.0, 100 mM NaCl, 2 mM EDTA, 0.5% Triton-X) for 1 min. The solution was centrifuged at 14,000*g* for 15 min at 4 °C and the resulting supernatant was subjected to a bead pull down assay.

One gram of cultured *Escherichia coli* cells expressing hnRNP A1-GST were resuspended in 5 ml of binding buffer (50 mM Tris–HCl, pH 8.0 containing 150 mM NaCl, 1 mM EDTA, 1 mM PMSF). Following sonication and centrifugation at 14,000*g* for 10 min at 4 °C, the supernatant was subjected to a bead pull down assay.

2.5. Pull down assay of hnRNP A1 protein from HeLa cell and *E. coli* soluble lysates

To remove the non-specific binders in soluble lysates, 500 μl of each soluble lysate was mixed with the 200 μl of avidin-agarose beads (Sigma-Aldrich) that were washed beforehand. After centrifugation at 14000 g for 15 min at 4 °C, the 90 μl of supernatant was mixed with 10 μl of 1 mM of CPT-20-B or DMSO (control) and incubated for 16 h at 4 °C with rotation. An aliquot of 200 μl of avidin-agarose beads (Sigma-Aldrich) were then added and incubated for 1 h at 4 °C to form avidin–biotin complex. After centrifugation at 14,000*g* for 10 min at 4 °C, the supernatant was removed and PBS was added to wash the beads. After washing the beads five times, the beads were mixed with SDS loading buffer (0.002% bromophenol blue, 0.002% xylene cyanol FF, 5% glycerol, 0.1% SDS) and incubated at 95 °C for 10 min. The resulting solution was subjected to SDS–PAGE using 15% polyacrylamide gel. The separated proteins were blotted onto PVDF membrane and hnRNP A1 protein was detected by western blot analysis using hnRNP A1 mouse monoclonal antibody (Santa Cruz Biotechnology Inc.) as a primary antibody and goat anti-mouse IgG antibody-AP conjugate (Nacalai Tesque). The chemiluminescence was performed using the CDP-Star Detection Reagent (GE Healthcare) to identify hnRNP A1.

2.6. Purification of recombinant protein

The recombinant hnRNP A1-GST was purified by an affinity chromatography using an FPLC system (ÄKTA explorer 10s, GE Healthcare) employing a GSTrap FF (1 ml) column. The soluble fraction of recombinant *E. coli* (PBS) was charged to the column and washed using PBS. The hnRNP A1-GST was then eluted using an elution buffer (50 mM phosphate, 150 mM NaCl, 10 mM glutathione, the reduced form, pH 8.0). The fractions were analyzed by SDS–PAGE using 10% separation gel and CBB staining. The fraction containing hnRNP A1-GST was desalted using PD-10 column (GE Healthcare) and then subjected to the interaction analysis.

The recombinant His-tagged cap region (215–433) of top I was purified by nickel affinity chromatography using Glutathione Sepharose™ 4B (2 ml) with an open column. The soluble fraction of recombinant *E. coli* (20 mM phosphate, 500 mM NaCl, 0.5 mM EDTA, 5 mM 2-mercaptoethanol (2-ME), pH 7.3) with protease inhibitor cocktail (Nacalai Tesque) was charged to the column and washed with 50 ml of buffer 1 (20 mM phosphate, 500 mM NaCl, 0.5 mM EDTA, 5 mM 2-ME, 5 mM $MgCl_2$, 0.5 M ATP, pH 7.3) and buffer 2 (20 mM phosphate, 2 M NaCl, 0.5 mM EDTA, 5 mM 2-ME, pH 7.3). The His-tagged protein was then eluted using 30 ml of an elution buffer (50 mM phosphate, 500 mM NaCl, 500 mM imidazole, pH 7.3). The purified protein was analyzed by SDS–PAGE using 12.5% separation gel and CBB staining. The fraction containing hnRNP A1-GST was desalted using PD-10 column (GE Healthcare) and then subjected to the interaction analysis.

2.7. Kinetic analysis using a QCM biosensor

Kinetic analysis was performed using a cuvette-type QCM device AffinixQ (Initium, Tokyo, Japan) and a ceramic sensor chip (Initium). The recombinant hnRNP A1-GST, which was purified by affinity chromatography, was immobilized on the gold electrode of a sensor chip. The sensor chip was then attached to the oscillator and immersed into the cuvette containing 8 ml of PBS–10% DMSO (25 °C). After stabilizing the QCM sensor, 8 μl of various concentrations (12.5, 25, 50, 100 and 250 μM) of CPT were injected into cuvette (final 12.5, 25, 50, 100 and 250 nM). The frequency change was then monitored until the sensor reached equilibrium. In total, three independent experiments were performed and kinetic parameters were calculated using AQUA 2.0 software. The data were analyzed as a Langumuir plot 1) (Fig. 2C) and a Scatchard plot 2) (Fig. 2D) using the following equations:

$$B_{eq} = \frac{B_{max} \cdot [CPT]}{K_D + [CPT]} \quad (1)$$

$$\frac{B_{eq}}{[CPT]} = \frac{B_{max}}{K_D} - \frac{1}{K_D} \cdot B_{eq} \quad (2)$$

where [CPT] is the concentration of CPT. B_{eq} is the response (Hz) at equilibrium between CPT and immobilized hnRNP A1-GST on a ceramic sensor chip. B_{max} is the maximum response (Hz); K_D is the dissociation constant between CPT and immobilized hnRNP A1-GST.

2.8. Kinetic analysis using a SPR biosensor

Analysis of binding between hnRNP A1-GST and His-tagged cap region (215–433) of top I, which were purified by FPLC, was performed with a surface plasmon resonance (SPR) biosensor (Biacore®3000, GE Healthcare). A surface of CM5 sensor chip was activated by injecting a solution containing 200 mM EDC and 50 mM NHS at 10 μl/min for 14 min. The His-tagged cap region protein (170 μl) in 10 mM acetate buffer (pH 5) was then injected over the sensor chip and captured on the carboxymethyl dextran matrix via an amine coupling reaction. The surface was then blocked by injecting 1 M ethanolamine at pH 8.5 for 14 min. This reaction immobilized about 10,000 resonance units (RU) of His-tagged cap region (215–433) of top I. Binding analysis was performed in HBS-EP buffer with 5% DMSO using a flow rate of 20 μl/min at 25 °C. Various concentrations of hnRNP A1-GST with or without of CPT were successively injected upon the immobilized His-tagged cap region to detect the SPR response generated by the hnRNP A1-GST binding.

The effect of CPT on hnRNP A1-cap region (215–433) interaction was elucidated by (3) Langmuir-plot and (4) Lineweaver-burk plot (Double-reciprocal plot) for a non-competitive inhibition model represented by the following equation:

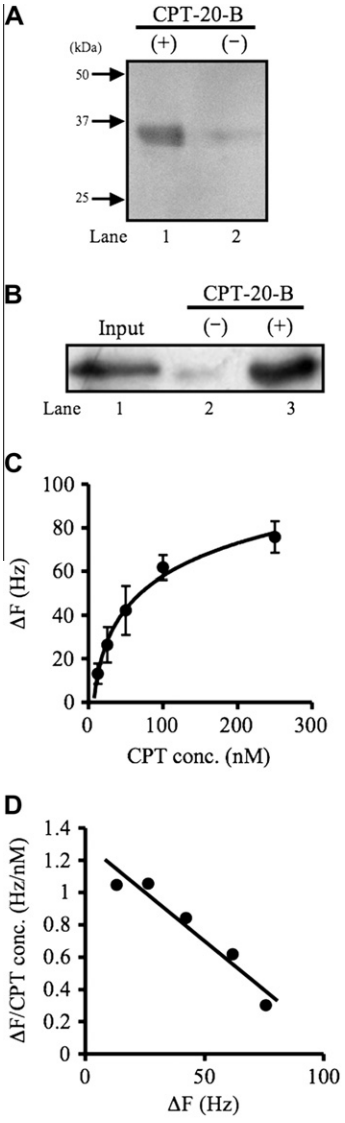

Figure 2. Direct interaction between CPT and hnRNP A1. (A, B) Extraction of CPT-20-B binding protein from a soluble fraction of HeLa cell (A) or recombinant *E. coli* (B). The 100 μM of CPT-20-B treated (+) or non-treated (−) avidin-agarose beads were incubated with the soluble fraction of HeLa cells. The resulting bead complex was centrifuged and treated with SDS sample buffer. After separation by SDS–PAGE, the proteins were blotted onto PVDF membrane and immunoblotted using an anti-hnRNP A1 monoclonal antibody. (C, D) Interaction analysis between CPT and recombinant hnRNP A1-GST using the QCM device. (C) Langmuir plot. The hnRNP A1-GST protein was immobilized onto the gold electrode of the sensor chip. After equilibration, the QCM sensor chip was immersed in a buffer-filled cuvette and a solution of CPT (12.5–250 μM) was injected (final concentration 12.5–250 nM). The subsequent frequency changes (ΔF) were then monitored. The data are means ± S.E. of three independent experiments. (D) Scatchard plot. 1 Hz = 0.62 pg/mm^2.

$$R_{eq} = \frac{R_{eq\,max}}{1 + \frac{[CPT]}{K_i}} \cdot \frac{1}{K_D + [hnRNPA1]} \cdot [hnRNP\ A1] \quad (3)$$

$$\frac{1}{R_{eq}} = \frac{K_D(1 + \frac{[CPT]}{K_i})}{R_{eq\,max}} \cdot \frac{1}{[hnRNPA1]} + \frac{1 + \frac{[CPT]}{K_i}}{R_{eq\,max}} \quad (4)$$

where hnRNP A1 is the concentration of protein; R_{eq} is the apparent response (RU) obtained from local fitting of SPR sensorgram between hnRNP A1 protein and cap region (215–433) on a CM5 sensor chip; $R_{eq\ max}$ is the maximum response (RU); K_D is the dissociation constant between hnRNP A1 and immobilized cap region (215–433); K_i is the dissociation constant between hnRNP A1 and CPT.

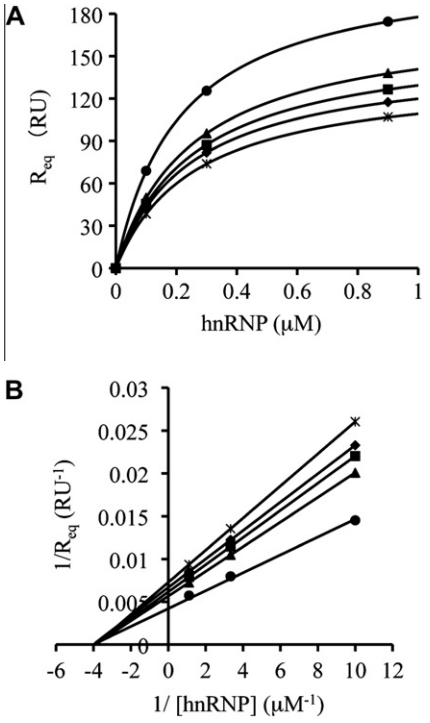

Figure 3. Effect of CPT for hnRNP A1/top I interaction on SPR analysis. (A) Langmuir plot. His-tagged cap region (215–433) of top I was immobilized on CM5 censor chip by an amine coupling reaction. The R_{eq} (RU) obtained local fitting for response upon injection of various concentration of hnRNP A1-GST with (0, 0.1, 0.3, 1 and 3 μM) CPT was plotted. (B) Lineweaver-burk (Double-reciprocal) plot. 1 RU = 1 pg/mm^2.

2.9. Drug evaluation using the *D. melanogaster*

Fly stocks were cultured at 25 °C on standard food. The Canton-S fly was used as the wild-type (WT) strain. A schematic representation of the drug evaluation protocol is shown in Figure 3A. Twenty adult *Drosophila* (10 males and 10 females) collected within 48 h after eclosion were raised and then their eggs collected during a 24 h period. The eggs were immersed in a 250 μl aliquot of CPT (0, 5, 12.5, 25 and 50 μM) dissolved in a solvent (4% EtOH, 5% DMSO). The number of adult *Drosophila* in each treated group [N (×μM)] that emerged within 15 days after administration of CPT was counted and compared to that of WT [N (0 μM)]. The eclosion rate [N (×μM)/N (0 μM) × 100%] was then calculated.

2.10. The supercoiled DNA relaxation assay

The supercoiled DNA relaxation by top I was detected according to the manufacture's instructions (TopoGEN Inc. Florida). Briefly, topoisomerase I (2 U) from calf thymus (TaKaRa Bio) was mixed with 1 μg of a supercoiled DNA pBR322 (TaKaRa Bio) in 20 μl of a reaction buffer (35 mM Tris–HCl, pH 8, 72 mM KCl, 5 mM $MgCl_2$, 5 mM DTT, 5 mM spermidine, 0.01% BSA) in the presence or absence of 100 μM CPT or 0.5 μM hnRNP A1-GST. The mixture was then incubated at 37 °C for 30 min. After the reaction, 2 μl of 10% SDS solution was added and incubated at 75 °C for 15 min to stop the reaction. By adding 2 μl of 0.6 μg/ml of proteinase K and incubating at 37 °C for 30 min, top I and hnRNP A1-GST were digested. The samples were subjected to 1% agarose gel electrophoresis and the gel was stained with 0.5 μg/ml ethidium bromide (EtBr).

3. Results

3.1. Similarity between a CPT-recognizing peptide and hnRNP A1

Previously, we identified a CPT-20-B (Fig. 1A) binding peptide, NSASRGGSQRGRGEH.[14] Our sequence analysis using the BLAST program also identified the S188–R196 region of hnRNP A1 as being quite similar to the peptide. As shown in Figure 1B and C, this segment corresponds to unstructured flexible loop region to the C-terminus of the RRM2 domain. This finding suggests that CPT may bind to hnRNP A1 via this portion. Interestingly it has been reported that hnRNP A1 directly bind to the cap region of human top I via two RRM domains and decrease CPT-induced DNA cleavage.[19–21] As shown in Figure 1D, the recombinant hnRNP A1-GST inhibited the DNA relaxation by top I regardless of the absence (lane 4) or presence (lane 5) of CPT, supporting the previous reports.[19–21]

3.2. Interaction between CPT and hnRNP A1 both in vivo and in vitro

A pull down assay using avidin-agarose beads and CPT-20-B was performed to test the direct interaction between CPT-20-B and hnRNP A1 in soluble fraction from the cells. As shown in Figure 2A and B, both native hnRNP A1 in HeLa cells and hnRNP A1-GST exogenously expressed in *E. coli* were pulled down from each cell lysate only in the presence of CPT-20-B.

Next, the dissociation constant between free CPT and the hnRNP A1-GST was elucidated using a QCM biosensor (AffinixQ, Initium).[22] The sensor chip, comprising a gold electrode onto which the recombinant hnRNP A1-GST protein was immobilized, was immersed in a buffer-filled cuvette. After stabilizing the QCM sensor, various concentrations (12.5–250 μM) of non-biotinylated CPT was successively injected into the cuvette (final concentration: 12.5–250 nM) and the frequency changes was monitored. As shown in Figure 2C, the change of QCM frequency increased in proportion to the increase in the concentration of CPT, demonstrating an interaction between immobilized hnRNP A1-GST and free CPT. From the Scatchard plot (Fig. 2D) using AQUA 2.0 software (Initium), the dissociation constant was calculated to be 82.7 nM, indicating a strong interaction between hnRNP A1 and CPT (Table 1). In addition, it was found that introduction of the biotin linker at position C20 of CPT does not interfere with its binding to hnRNP A1.

3.3. CPT non-competitively inhibits hnRNP A1/top I interaction

To ascertain the effect for binding of CPT to hnRNP A1, we elucidated the hnRNP A1/top I association in the presence or absence of CPT using a surface plasmon resonance (SPR) biosensor (Biacore®3000, GE Healthcare). RRM proteins including hnRNP A1 directly bind to top I via two tandem RRM domains.[19–21] To avoid the binding of CPT to the DNA-binding domain in top I, we engineered a deletion mutant that corresponds to the cap region (215–433) of top I and used for analysis. As shown in Figure 3A, hnRNPA1-GST bound to the cap region (215–433) of top I immobilized on CM5 sensor chip on a dose dependent manner, yielding the K_D value of 260 nM (Table 1, Supplementary Fig. 1A). This response reduced in proportion to the increase of CPT concentration (Fig. 3A and Supplementary Fig. 1B–D), suggesting that CPT inhibits the binding of hnRNP A1 to top I. CPT itself did not show any response against cap region (215–433) of top I up to 0.9 μM (Supplementary Fig. 1E). The Lineweaver-burk plot (Fig. 3B) and subsequent kinetic analysis revealed the reduction of $R_{eq\ max}$, but not change the K_D value, which indicates that CPT non-competitively interferes the formation of hnRNP A1/top I complex. Taken together with the result of pull down assay and QCM analysis, it is suggested that CPT directly binds to hnRNP A1 and non-competitively inhibits the hnRNP A1/top I interaction.

Table 1
Kinetic parameters of the interaction between hnRNP A1 and CPT or cap region of top I

	K_D (nM)	B_{max} (pg/mm^2)
hnRNP A1-CPT	82.7	67
hnRNP A1-top I	260	238

The data was obtained from QCM (hnRNP A1-CPT) or SPR (hnRNP A1-top I) analysis. AQUA 2.0 software (Initium) or BIAevaluation 4.1 software (GE Healthcare) was used to calculate the dissociation constant.

3.4. Elucidation of the change of growth inhibitory effect of CPT in vivo by the use of a *Drosophila*-based drug evaluation system

To elucidate the change of growth inhibitory effect of CPT by knockout of the *hnRNP A1* gene in vivo, we used a drug evaluation system using *Drosophila melanogaster* (Fig. 4A) and assessed the effect of CPT in the presence or absence of *Hrb87F* (a homolog of *hnRNP A1*) gene expression.[23] Indeed, Hrb87F of *D. melanogaster* displays homology with hnRNP A1 (data not shown). The 15-mer CPT recognizing peptide also showed similarity with the unstructured flexible loop on the C-terminal side of the RRM2 domain of Hrb87F (Fig. 1B and C). As shown in Figure 4B, administration of CPT revealed the sensitization of the growth inhibitory effect of CPT against the *Hrb87F* mutants in a concentration-dependent manner. This effect was similarly observed on two other drosophila strain $Hrb87F^{KG02089}$ and $Hrb87F^{BG02743}$ (Fig. 4C). In particular, administration of 25 or 50 μM of CPT was fatal to 7-day-old pupa of both $Hrb87F^{KG02089}$ and $Hrb87F^{BG02743}$ (Fig. 4D). By contrast, there was little difference of eclosion rates and phenotypic observations without treatment of CPT among the flies tested. Taken together, these data suggest that knockout of the *Hrb87F* gene sensitizes the growth inhibitory effect of CPT and is fatal above 25 μM at pupa stage.

To further evaluate the susceptibility of CPT on Hrb87F mutants, we tested several cytotoxic drugs (paclitaxel, irinotecan, doxorubicin, bleomycin and cysplatin) in addition to CPT. Figure 4E shows the eclosion rate of $Hrb87F^{KG02089}$ mutant after administration of each drug. Interestingly, the administration of 25 μM of each drug other than CPT did not show any effect on eclosion of the *Hrb87F* gene mutant strain. This result indicates that susceptibility of the growth inhibitory effect by the knockout of *Hrb87F* is specific for CPT.

4. Discussion

The drug-recognizing peptide sequence identified by the phage display technology enables combinatorial discovery of drug-binding target.[24] In particular, phage-displayed short peptide indicates disordered loop within proteins,[25,26] which has recently been suggested to be an essential observation when considering the drug/protein interactions.[27–29] Indeed, we have identified several drug/protein interactions that point out such properties.[30–34] As for the CPT, the 15-mer peptide showed the similarity against not only the CPT-binding site in top I,[14] but also the unstructured flexible loop positioned to the C-terminus of the RRM2 domain in hnRNP A1 (Fig. 1B and C). Indeed, binding assays demonstrated that CPT binds to hnRNP A1 both in vitro and in vivo. Furthermore, the direct interaction between tandem RRMs in hnRNP A1 and cap region (215–433) of top I (K_D: 260 nM), which is approximately three-fold weaker than that between CPT and hnRNP A1

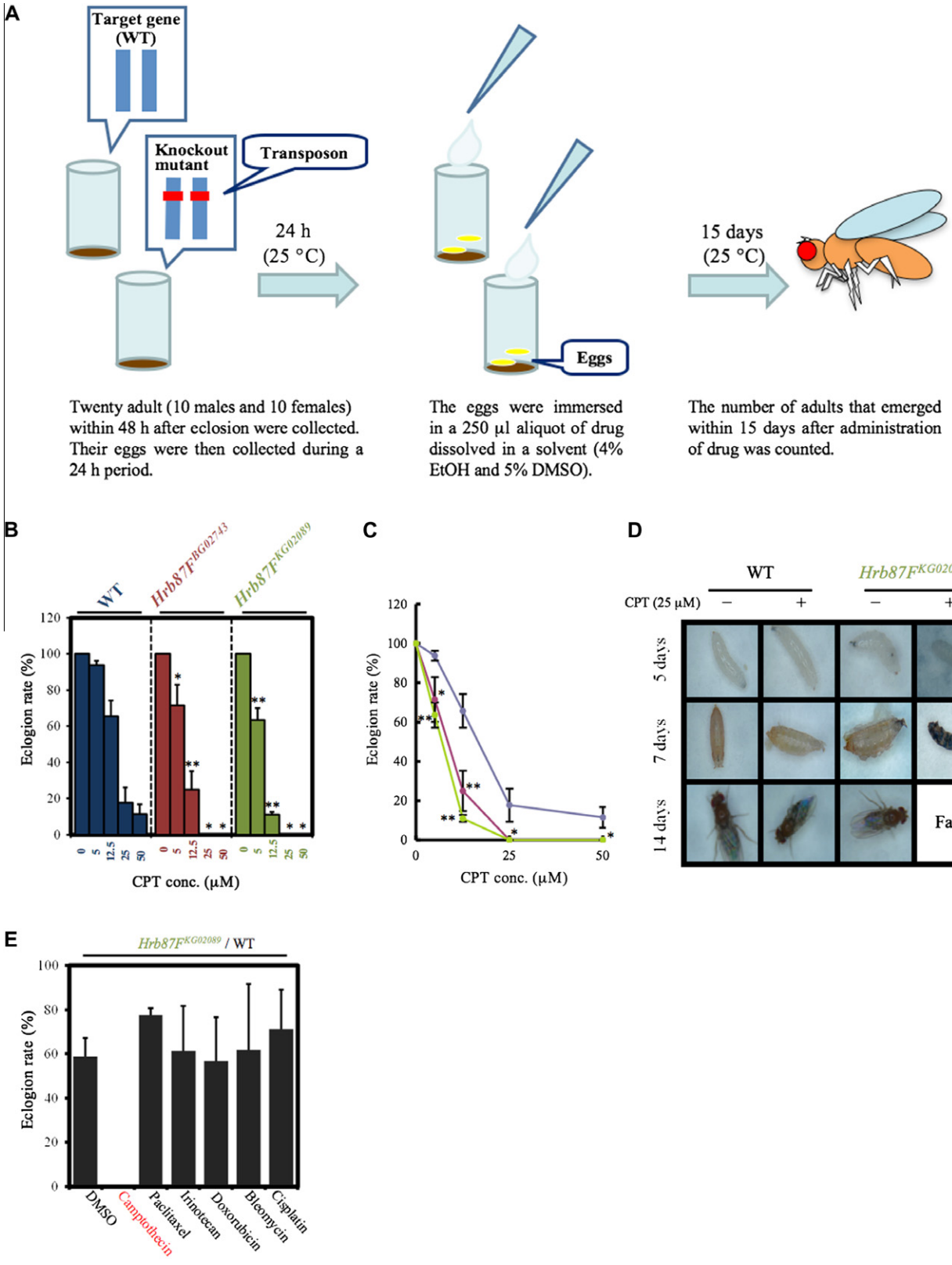

Figure 4. Drug evaluation using *D. melanogaster*. (A) Schematic representation of the procedure employed for the drug-sensitivity test using *D. melanogaster*. (B, C) CPT susceptibility test using *Hrb87F* gene mutant and WT strains. The number of adults that emerged from a pupa after treatment with each concentration of CPT (×µM) was compared to that of 0 µM and shown as an eclosion rate [N (×µM)/N (0 µM) × 100%]. WT: blue bar or line [N_{means} = 179 (0 µM of CPT), 168 (5 µM), 118 (12.5 µM), 32 (25 µM), 21 (50 µM)], $Hrb87F^{BG02743}$: red bar or line [N_{means} = 52 (0 µM), 37 (5 µM), 14 (12.5 µM), 0 (25 µM), 0 (50 µM)], $Hrb87F^{KG02089}$: green bar or line [N_{means} = 81 (0 µM), 52 (5 µM), 9 (12.5 µM), 0 (25 µM), 0 (50 µM)]. The data are means ± S. E. of three independent experiments. $^{*}P$ <0.05, $^{**}P$ <0.01 versus WT. (D) The phenotypic change of WT and *Hrb87F* mutant strains at 5, 7 and 14 days after administration of 25 µM of CPT. (E) Selective susceptibility of CPT against the *Hrb87F* mutant strain $Hrb87F^{KG02089}$. The 25 µM of each drug was administrated and the eclosion rate calculated [N ($Hrb87F^{KG02089}$)/N (WT) × 100%]. WT: N_{means} = 163 (DMSO), 80 (CPT), 125 (paclitaxel), 167 (irinotecan), 133 (doxorubicin), 103 (bleomycin), 135 (cisplatin), $Hrb87F^{KG02089}$: N_{means} = 95 (DMSO), 0 (CPT), 97 (paclitaxel), 100 (irinotecan), 73 (doxorubicin), 58 (bleomycin), 93 (cisplatin). The data are means ± S.E. of three independent experiments.

(K_D: 82.7 nM), was inhibited in the presence of CPT in a non-competitive manner (Fig. 3). These data are consistent with the fact that CPT binds to the unstructured portion but not to RRMs (Fig. 1B and C), which might arise conformational change of RRMs and allosterically inhibit the hnRNP A1/top I interaction. We tried to detect the structural changes of hnRNP A1 in the presence or absence of CPT using the measurement of circular dichroism (CD). However, it was somewhat challenging because CPT alone affected the CD spectra.

By contrast, we assessed the biological effect of CPT targeting the hnRNP A1/top I interaction using Drosophila-based drug evaluation system. The use of *D. melanogaster* is a potentially effective means of evaluating a drug of interest and provides a higher throughput rate than conventional approaches using mammals.[35–38] In addition to the abundance of genomic information and availability of a knockout library,[39] approximately 75% of the genome is conserved between *Drosophila* and humans.[35] In this study, the *Hrb87F* gene (hnRNP A1 homolog) knockout strains clearly showed the susceptibility for the growth inhibitory effect specific for CPT (Fig. 4). As reported previously, RRM proteins themselves could regulate the activity of top I.[19–21] The knockout strain of *D. melanogaster* loses the Hrb87F as a naïve top I regulator and subsequently enhances the relative DNA relaxation by top I. As compared to wild-type strain (Fig. 5A), Hrb87F knockout strain may easily form CPT-top I-DNA complexes under the same concentration of CPT (Fig. 5B). Furthermore, because CPT itself shows strong affinity with hnRNP A1 (K_D: 82.7 nM), which is approximately two order magnitudes higher than that for 50% of top I inhibitory concentration (submicromolar), the knockout of Hrb87F causes defect of CPT-binding site and probabilistically increases the action of CPT toward to top I, resulting in enhancement of the growth inhibitory effect in vivo.

Recently, spliceostatin, a methylated derivative of natural product FR901464, has been reported as a first anti-tumor compound that inhibits pre-mRNA splicing by targeting SF3b in spliceosome.[40] We have not still elucidated the effect of CPT/hnRNP A1 interaction for pre-mRNA splicing or RNA metabolism. Nontheless, it was reported that CPT treatment amplifies splicing factor signals by stalling nascent RNPs and giving the nascent RNA more time to bind splicing factors, indicating the direct relevance of CPT for RNA splicing.[41] The binding of CPT to hnRNP A1, which has been identified in this study, should also become a sound platform to elucidate the mode of action of CPT for pre-mRNA splicing in the nucleus.

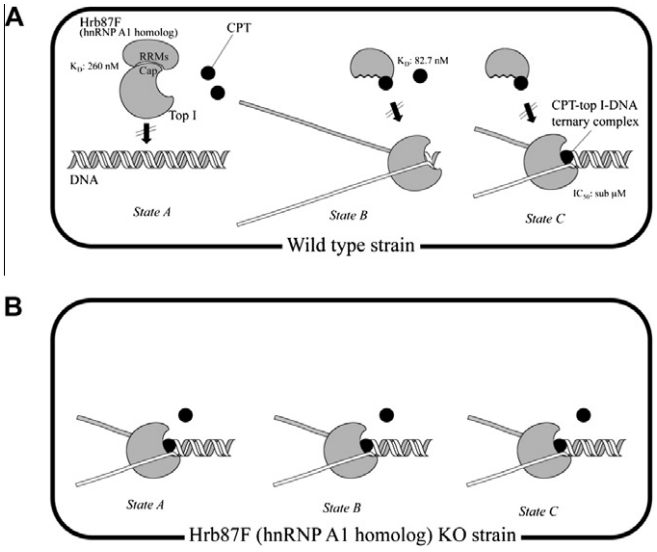

Figure 5. Possible state of CPT in Drosophila. (A) Wild-type strain. State A; the formation of hnRNP A1-Top I complex. Top I is not capable of binding to DNA during the hnRNP A1 association.[19–21] States B and C; allosteric inhibition of hnRNP A1/top I interaction by CPT. Top I can unwind the double-stranded DNA (State B) or form CPT-top I-DNA ternary complex (State C) that causes growth inhibitory effect. (B) The *Hrb87F* knockout strain. The absence of Hrb87F allows binding of top I to DNA and increases the formation of CPT-top I-DNA ternary complexes.

Acknowledgments

We thank Yakult Co. Ltd. (Tokyo, Japan) and Dai-ichi Pharmaceutical Co. Ltd. (Tokyo, Japan) for providing irinotecan. We also thank the Bloomington Stock Center for the fly stocks. This work was partially supported by a Grant-in-Aid for Scientific Research (The Ministry of Education, Culture, Sports, Science and Technology of Japan, Japan Society for the Promotion of Science).

Supplementary data

Supplementary data associated with this article can be found, in the online version, at doi:10.1016/j.bmc.2011.09.059.

References and notes

1. Wall, M. E.; Wani, M. C.; Cook, C. E.; Palmer, K. H.; McPhail, H. T.; Sim, G. A. *J. Am. Chem. Soc.* **1966**, *88*, 3888.
2. Hsiang, Y. H.; Liu, L. F. *Cancer Res.* **1988**, *48*, 1722.
3. Hsiang, Y. H.; Hertzberg, R.; Hecht, S.; Liu, L. F. *J. Biol. Chem.* **1985**, *260*, 14873.
4. Verbiest, V.; Montaudon, D.; Tautu, M. T.; Moukarzel, J.; Portail, J. P.; Markovits, J.; Robert, J.; Ichas, F.; Pourquier, P. *FEBS Lett.* **2008**, *582*, 1483.
5. Reuveni, D.; Halperin, D.; Shalit, I.; Priel, E.; Fabian, I. *Biochem. Pharmacol.* **2008**, *75*, 1272.
6. Croce, A. C.; Bottiroli, G.; Supino, R.; Favini, E.; Zuco, V.; Zunino, F. *Biochem. Pharmacol.* **2004**, *67*, 1035.
7. Rapisarda, A.; Uranchimeg, B.; Scudiero, D. A.; Selby, M.; Sausville, E. A.; Shoemaker, R. H.; Melillo, G. *Cancer Res.* **2002**, *62*, 4316.
8. Motwani, M.; Sirotnak, F. M.; She, Y.; Commes, T.; Schwartz, G. K. *Cancer Res.* **2002**, *62*, 3950.
9. Blandizzi, C.; De Paolis, B.; Colucci, R.; Lazzeri, G.; Baschiera, F.; Del Tacca, M. *Br. J. Pharmacol.* **2001**, *132*, 73.
10. Walowsky, C.; Fitzhugh, D. J.; Castano, I. B.; Ju, J. Y.; Levin, N. A.; Christman, M. F. *J. Biol. Chem.* **1999**, *274*, 7302.
11. Hecht, J. R. *Oncology (Williston Park)* **1998**, *12*, 72.
12. Sakai, H.; Sato, T.; Hamada, N.; Yasue, M.; Ikari, A.; Kakinoki, B.; Takeguchi, N. *J. Physiol.* **1997**, *505*, 133.
13. Sakai, H.; Diener, M.; Gartmann, V.; Takeguchi, N. *Naunyn Schmiedebergs Arch. Pharmacol.* **1995**, *351*, 309.
14. Takakusagi, Y.; Takakusagi, K.; Kuramochi, K.; Kobayashi, S.; Sugawara, F.; Sakaguchi, K. *Bioorg. Med. Chem.* **2007**, *15*, 7590.
15. Takakusagi, Y.; Ohta, K.; Kuramochi, K.; Morohashi, K.; Kobayashi, S.; Sakaguchi, K.; Sugawara, F. *Bioorg. Med. Chem. Lett.* **2005**, *15*, 4846.
16. Li, X. G.; Haluska, P., Jr.; Hsiang, Y. H.; Bharti, A. K.; Kufe, D. W.; Liu, L. F.; Rubin, E. H. *Biochem. Pharmacol.* **1997**, *53*, 1019.
17. Munroe, S. H.; Dong, X. F. *Proc. Natl. Acad. Sci. U.S.A.* **1992**, *89*, 895.
18. Pontius, B. W.; Berg, P. *Proc. Natl. Acad. Sci. U.S.A.* **1990**, *87*, 8403.
19. Trzcinska-Daneluti, A. M.; Gorecki, A.; Czubaty, A.; Kowalska-Loth, B.; Girstun, A.; Murawska, M.; Lesyng, B.; Staron, K. *J. Mol. Biol.* **2007**, *369*, 1098.
20. Kowalska-Loth, B.; Girstun, A.; Trzcinska, A. M.; Piekielko-Witkowska, A.; Staron, K. *Biochem. Biophys. Res. Commun.* **2005**, *331*, 398.
21. Kowalska-Loth, B.; Girstun, A.; Piekielko, A.; Staron, K. *Eur. J. Biochem.* **2002**, *269*, 3504.
22. Takakusagi, Y.; Kobayashi, S.; Sugawara, F. *Bioorg. Med. Chem. Lett.* **2005**, *15*, 4850.
23. Haynes, S. R.; Johnson, D.; Raychaudhuri, G.; Beyer, A. L. *Nucleic Acids Res.* **1991**, *19*, 25.
24. Takakusagi, Y.; Takakusagi, K.; Sugawara, F.; Sakaguchi, K. *Expert Opin. Drug Discov.* **2010**, *5*, 361.
25. Rodi, D. J.; Agoston, G. E.; Manon, R.; Lapcevich, R.; Green, S. J.; Makowski, L. *Comb. Chem. High Throughput Screen.* **2001**, *4*, 553.
26. Rodi, D. J.; Janes, R. W.; Sanganee, H. J.; Holton, R. A.; Wallace, B. A.; Makowski, L. *J. Mol. Biol.* **1999**, *285*, 197.
27. Brown, C. J.; Johnson, A. K.; Dunker, A. K.; Daughdrill, G. W. *Curr. Opin. Struct. Biol.* **2011**, *21*, 441.
28. Uversky, V. N.; Dunker, A. K. *Biochim. Biophys. Acta* **2010**, *1804*, 1231.
29. Metallo, S. J. *Curr. Opin. Chem. Biol.* **2010**, *14*, 481.
30. Takami, M.; Takakusagi, Y.; Kuramochi, K.; Tsukuda, S.; Aoki, S.; Morohashi, K.; Ohta, K.; Kobayashi, S.; Sakaguchi, K.; Sugawara, F. *Molecules* **2011**, *16*, 4278.
31. Takakusagi, K.; Takakusagi, Y.; Ohta, K.; Aoki, S.; Sugawara, F.; Sakaguchi, K. *Protein Eng. Des. Sel.* **2010**, *23*, 51.

32. Nishiyama, K.; Takakusagi, Y.; Kusayanagi, T.; Matsumoto, Y.; Habu, S.; Kuramochi, K.; Sugawara, F.; Sakaguchi, K.; Takahashi, H.; Natsugari, H.; Kobayashi, S. *Bioorg. Med. Chem.* **2009**, *17*, 195.
33. Takakusagi, Y.; Kuroiwa, Y.; Sugawara, F.; Sakaguchi, K. *Bioorg. Med. Chem.* **2008**, *16*, 7410.
34. Aoki, S.; Morohashi, K.; Sunoki, T.; Kuramochi, K.; Kobayashi, S.; Sugawara, F. *Bioconjug. Chem.* **2007**, *18*, 1981.
35. Pandey, U. B.; Nichols, C. D. *Pharmacol. Rev.* **2011**, *63*, 411.
36. Avanesian, A.; Semnani, S.; Jafari, M. *Drug Discov. Today* **2009**, *14*, 761.
37. Tickoo, S.; Russell, S. *Curr. Opin. Pharmacol.* **2002**, *2*, 555.
38. Reiter, L. T.; Bier, E. *Expert Opin. Ther. Targets* **2002**, *6*, 387.
39. Yamazaki, Y.; Akashi, R.; Banno, Y.; Endo, T.; Ezura, H.; Fukami-Kobayashi, K.; Inaba, K.; Isa, T.; Kamei, K.; Kasai, F.; Kobayashi, M.; Kurata, N.; Kusaba, M.; Matuzawa, T.; Mitani, S.; Nakamura, T.; Nakamura, Y.; Nakatsuji, N.; Naruse, K.; Niki, H.; Nitasaka, E.; Obata, Y.; Okamoto, H.; Okuma, M.; Sato, K.; Serikawa, T.; Shiroishi, T.; Sugawara, H.; Urushibara, H.; Yamamoto, M.; Yaoita, Y.; Yoshiki, A.; Kohara, Y. *Nucleic Acids Res.* **2010**, *38*, D26.
40. Kaida, D.; Motoyoshi, H.; Tashiro, E.; Nojima, T.; Hagiwara, M.; Ishigami, K.; Watanabe, H.; Kitahara, T.; Yoshida, T.; Nakajima, H.; Tani, T.; Horinouchi, S.; Yoshida, M. *Nat. Chem. Biol.* **2007**, *3*, 576.
41. Listerman, I.; Sapra, A. K.; Neugebauer, K. M. *Nat. Struct. Mol. Biol.* **2006**, *13*, 815.